Fabrication of sponge biomass adsorbent through UV-induced surface-initiated polymerization for the adsorption of Ce(III) from wastewater

Chen Liu, Chunjie Yan, Sen Zhou and Wen Ge

ABSTRACT

The recovery of rare earth ions from industrial wastewater has aroused wide concern in recent years. In present work, we synthesized a novel three-dimensional adsorbent (denoted as LF-AA) by grafting loofah fiber with acrylic acid via ultraviolet radiation. The LF-AA was washed by boiling water and subjected to soxhlet extraction with acetone and then fully characterized by attenuated total reflectance Fourier transform infrared spectroscopy (ATR-FTIR) and scanning electron microscopy (SEM). Rare earth ion (Ce(III)) was selected as a model to validate its adsorption property. The saturation adsorption capacity for Ce(III) reaches 527.5 mg/g. Not only was this material highly efficient at adsorbing Ce(III) from aqueous solutions, it also proved to have ideal performance in regeneration; the total adsorption capacity of LF-AA for Ce(III) after six successive cycles decreased only 6.40% compared with the initial capacity of LF-AA. More importantly, the LF-AA can be easily separated from aqueous solutions because of its three-dimensional sponge natural structure. This study provides a new insight into the fabrication of biomass adsorbent and demonstrated that the LF-AA can be used as excellent adsorbent for the recovery of rare earth ions from wastewater.

Key words | biomass adsorbent, Ce(III) adsorption, recycling, surface modification, wastewater treatment

Chen Liu
Chunjie Yan (corresponding author)
Sen Zhou
Wen Ge
Faculty of Material and Chemistry,
China University of Geosciences,
Lu Mo Road 388,
Wuhan 430074,
China
E-mail: *chjyan2005@126.com*

Chen Liu
Chunjie Yan
Engineering Research Center of Nano-Geomaterials,
Ministry of Education, China University of Geosciences,
Lu Mo Road 388,
Wuhan 430074,
China

INTRODUCTION

Rare earth elements (REEs) are becoming one of the most important and indispensable strategic resources in the development of advanced materials science, due to their outstanding physical, chemical and nuclear properties (Uda *et al.* 2000; Chen 2011; Jordens *et al.* 2013; Madhukar Reddy *et al.* 2015). However, abundant wastewater containing rare earth ions is produced in rare earth separation and extraction processes. The REEs concentrations of wastewaters from rare earth smelting enterprises ranged from 150.0 mg/L to 300.0 mg/L according to our investigations. This means that rare earth resources are heavily wasted with the wastewater discharged (Wübbeke 2013; Yang *et al.* 2013). Although REEs are not typically considered water contaminants, it has been reported that REEs have many toxic effects in bacteria (GAO *et al.* 2015), plants (Brioschi *et al.* 2013), animals (Feng *et al.* 2006; Zhao *et al.* 2011) and human beings (Fan *et al.* 2004; Babula *et al.* 2008; Liu *et al.* 2014). Therefore, it is of great realistic significance to recycle rare earth ions from the waste water (Wu *et al.* 2012).

Up to now, various technologies have been developed for the effective recovery of rare earth ions, such as chemistry precipitation, solvent extraction, reverse osmosis, adsorption or ion-exchange and so on (Xie *et al.* 2014). However, most of these methods are usually of poor efficiency, high cost and generation of secondary contamination (Binnemans *et al.* 2013). Adsorption, with advantages of low investment, high efficiency and easy operation, is considered to be the most reliable treatment approach for the recovery of REEs from aqueous solutions. The commercially used adsorbent for rare earth ions removal is ion exchange resin, which is costly and produced with unsustainable fossil raw material. Many other novel adsorbents were also tested, such as clay minerals (attapulgite, diatomite), alumina, iron(III) hydroxide and active carbon. However, the main shortcomings of these adsorbents are poor physical strength, low adsorption

doi: 10.2166/wst.2017.144

capacities or not ideal performance in regeneration (Zhou *et al.* 2014). Consequently, it is quite necessary to develop new types of highly efficient adsorbents.

Recently, the use of low cost, renewable and biodegradable agricultural and forest residues, such as biomass fiber, in the development of novel adsorbents has drawn wide attention due to increasing concern over environmental protection and sustainable development (Basha *et al.* 2009; Hameed & Ahmad 2009; Bilal *et al.* 2013). There are many methods in the development of biomass adsorbents, such as heat-treatment to preparation of activated carbon, acid or alkali treatment, grafting polymers, loaded with metal oxides and coating organic compounds. Among them, UV-induced surface-initiated polymerization as well as grafting polymer is considered to be one of the most effective measures to improve adsorption capacity of biomass materials (Zhou *et al.* 2016b). Loofah sponge fiber (LF), fruit of luffa cylindrical plants with three-dimensional natural structure, has been proved to have excellent mechanical properties and versatile surface chemistry. Recently, increasing attention has been focused on the modification of LF, especially in the fields of new energy, biofuel cells, supercapacitors and dye/metal cation removal process (Altinisik *et al.* 2010; Yuan *et al.* 2013; Li *et al.* 2014; Thakur & Thakur 2014; Liu *et al.* 2015). However, natural LF mainly consists of cellulose, hemicelluloses and lignin (Ghali *et al.* 2009), indicating that it has no functional groups which can work in metal cations adsorption process. Therefore, grafting LF with functional groups is of great significance in wastewater treatment. Poly(acrylic acid) has an advantage in adsorption due to the numerous carboxyl groups, but the polymer structure of poly(acrylic acid) can be easily destroyed by boiling water or organic solvent. Therefore, single poly (acrylic acid) without stable structure is not an ideal adsorbent for heavy metal ions removal from wastewater.

Considering the outstanding properties and special structure of LF, and excellent adsorption capacity of poly (acrylic acid) (PAA), in this paper a novel biomass adsorbent (LF-AA) was prepared by grafting loofah sponge fiber with acrylic acid (AA) via ultraviolet radiation grafting route. Rare earth ion (Ce(III)) was selected as a model to validate the adsorption property of LF-AA. We focused on the objectives: (1) to characterize physicochemical structure of LF-AA by scanning electron microscopy (SEM) and attenuated total reflectance Fourier transform infrared spectroscopy (ATR-FTIR); (2) to investigate the adsorption behavior of LF-AA for Ce(III) (i.e. effects of grafting yield, pH, ionic strength, adsorption kinetics and isotherms); (3) to evaluate the desorption and regeneration performance of LF-AA.

MATERIAL AND METHODS

Chemicals and materials

Acrylic acid (AA, monomer), benzophenone (BP, photosensitizer), acetone (ACE), sodium chloride (NaCl), and $Ce(NO_3)_3{\cdot}6H_2O$ were purchased from Sinopharm Chemical Reagent Co., Ltd (Shanghai, China). The stock solution of Ce(III) used in this study was prepared by dissolving $Ce(NO_3)_3{\cdot}6H_2O$ in double distilled water. All substances were analytical grade and used without further purification.

Loofah sponge fiber was obtained from Hubei province, China. Protogenic loofah sponge fiber was cooked by boiling water for 30 min after cutting into strips, then washed with distilled water and dried under 333.15 K in vacuum environment for subsequent use.

Preparation of LF-AA

The LF-AA was prepared in two steps, as shown in Figure 1. Firstly, the LF&BP was prepared by soaking LF in BP solution of ethanol. Typically, the LF&BP was obtained by adding LF strip into 25 mL of 0.1 wt.% BP solution of ethanol and then drying at 323.15 K. Secondly, the graft polymerization of LF&BP was achieved by the hydrogen abstraction reaction of AA and LF via ultraviolet radiation grafting route. In a typical reaction, one strip of LF&BP (with a total weight of about 1.0 g) was introduced in 25 mL of water, and AA solution (5 mL in 50 mL water) was added into a quartz tube, ensuring the LF was immersed in AA solution, and then the polymer grafting occurred by the UV-irradiation (UV lamp, power of 7 W, wavelength of 254 nm) for 6 h. Afterwards, the product was washed by boiling water and subjected to soxhlet extraction with acetone for 24 h to remove the homopolymers likely to be formed. Finally, the product (LF-AA) was dried in a vacuum oven at 333.15 K.

Characterization

Observations of the morphology of LF and LF-AA were characterized by field emission scanning electron microscope (FE-SEM) (SU8010, Hitachi, Ltd, Japan). The surface functional groups of LF and LF-AA were detected by FTIR (Nicolet iS50, Thermo Fisher Scientific Inc., USA), where the spectra were performed by ATR and recorded from 4,000 to 400 cm^{-1}.

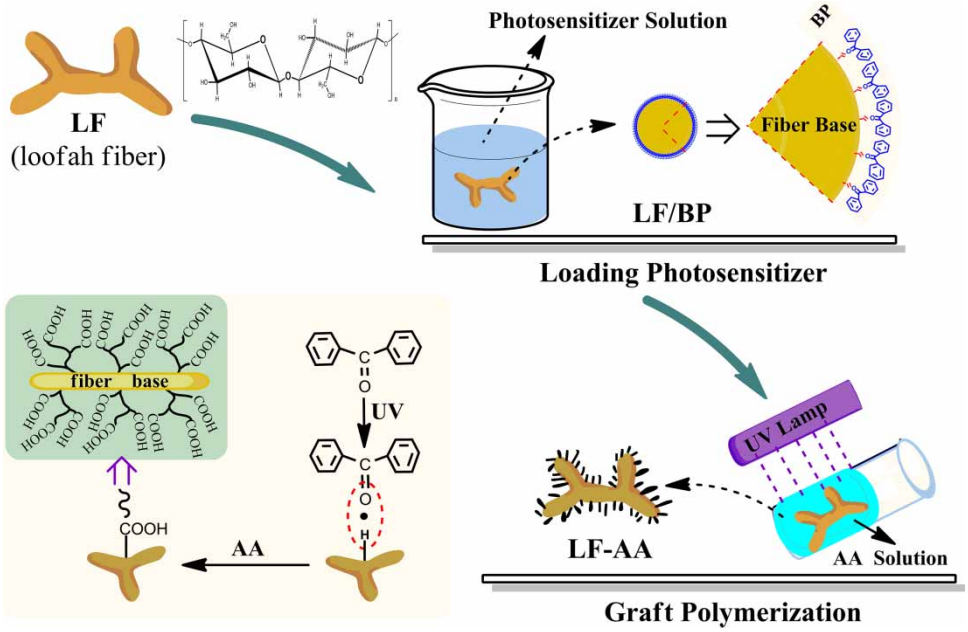

Figure 1 | Scheme of preparation of LF-AA composite.

Batch adsorption experiments

The Ce(III) adsorption properties of LF-AA were primarily evaluated by using a batch adsorption experiment. Typically, 20 mL of Ce(III) solution with desired concentration and 10 mg of LF-AA were added to a vial and then shaken with a speed of 150 shakes·min^{-1} in a thermostat shaker at 303.15 K for 4 h. Then the adsorbent was separated and the composition of solutions was determined by ICP (DGS-III, Shanghai Tailun Spectrometry Co. Ltd, China) to monitor the change of Ce(III) concentration before and after adsorption. The effect of pH on Ce(III) was adjusted in the range from 1.0 to 6.0 and maintained by 1 M NaOH or HCl, respectively. The effect of ionic strength (NaCl) was also studied by adjusted solution at various Ce(III) concentrations (50–500 mg/L) and different ionic strength (1–80 mmol/L) at optimal pH. The adsorption kinetic was conducted at three initial Ce(III) concentrations (100, 200 and 300 mg/L) by varying the contact time from 5 to 300 minutes at optimal pH. The adsorption isotherm on the adsorption of LF-AA toward Ce(III) was studied with a range of initial Ce(III) concentrations at optimal pH from 50 to 400 mg/L at 303.15, 313.15 and 323.15 K, respectively. The adsorption capacity was calculated as follows:

$$q_e = \frac{(C_0 - C_e)V}{m} \tag{1}$$

where q_e (mg/g) is the adsorption capacity of Ce(III) at equilibrium, V (L) is the volume of solution and m (g) is the amount of adsorbent, C_0 (mg/L) and C_e (mg/L) are the concentrations of Ce(III) at initial and equilibrium, respectively.

Reusability of LF-AA

To evaluate the reusability of LF-AA, a set of adsorption/desorption was performed. Typically, 10 mg of LF-AA was added to 20 mL of Ce(III) solution (300 mg/L), and the mixture was shaken in a shaker at 150 shake·min^{-1} for 4 h. Then the Ce(III)-adsorbed LF-AA was separated and desorbed by being dispersed into 0.2 M HCl to be shaken for 4 h. After desorption, the LF-AA was separated and activated by 2% NaOH solution for 15 min, then washed with distilled water to neutralize for the next cycle.

The desorption rate was calculated as follows:

$$\text{Desorption rate } (\%) = \frac{C_n V}{m q_{n-1}} \times 100\% \tag{2}$$

where m (g) is the quality of the adsorbent, q_n (mg/g) is the situated adsorption capacity and C_n (mg/L) is the equilibrium concentration of Ce(III) at regeneration cycle time n, V (L) is the volume of the solution.

Theory

To further investigate the adsorption efficiency of the adsorbent, the pseudo-first-order (Equation (3)) and pseudo-second-order (Equation (4)) rate equations were evaluated based on the experimental data.

$$q_t = q_e\left(1 - e^{-k_1 t}\right) \tag{3}$$

$$q_t = \frac{k_2 q_e^2 t}{1 + k_2 q_e t} \tag{4}$$

where q_t (mg/g) is the adsorption capacity at time t (min); q_e (mg/g) is the adsorption capacity at adsorption equilibrium; k_1 (min^{-1}) is the kinetic rate constant of the pseudo-first-order, and k_2 ($g{\cdot}mg^{-1}{\cdot}min^{-1}$) is the kinetic rate constant of the pseudo-second-order model.

The equilibrium adsorption data are analyzed by fitting them to Langmuir (Langmuir 1917) and Freundlich (Jaroniec *et al.* 1983) models, expressed by Equations (5) and (6), respectively.

$$q_e = \frac{q_m K_L C_e}{1 + K_L C_e} \tag{5}$$

$$q_e = K_F C_e^{1/n} \tag{6}$$

where C_e is the equilibrium concentration of Ce(III) (mg/L), q_e (mg/g) is the adsorption capacity at adsorption equilibrium; q_m is the maximum adsorption capacity (mg/g), K_L (L/mg) is the Langmuir isotherm constant; K_F ($mg^{1-1/n}{\cdot}L^{1/n}{\cdot}g^{-1}$) and n are Freundlich constants representing adsorption capacity and adsorption intensity, respectively.

RESULTS AND DISCUSSION

Characterization of adsorbent

Figure 2 shows the SEM images of LF and LF-AA. We observed that LF-AA (Figure 2(c)) keeps the basic structure of raw LF (Figure 2(a)). The significant difference is the surface morphology; the LF (Figure 2(b)) has a rough surface without shiny look and just like a dry branch, while the surface of LF-AA (Figure 2(d)) is full of smooth bumps and pronounced pleats, indicating that the LF has been successfully modified by PAA (Karlsson *et al.* 2000; Henriksson & Gatenholm 2002; Kato *et al.* 2003).

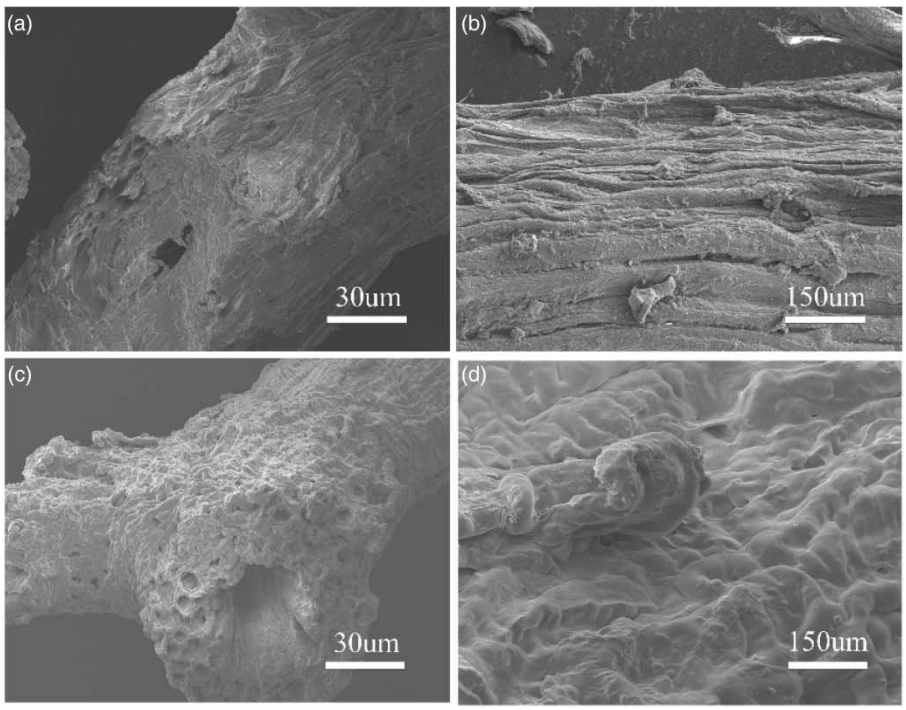

Figure 2 | The SEM image of (a), (b) LF and (c), (d) LF-AA.

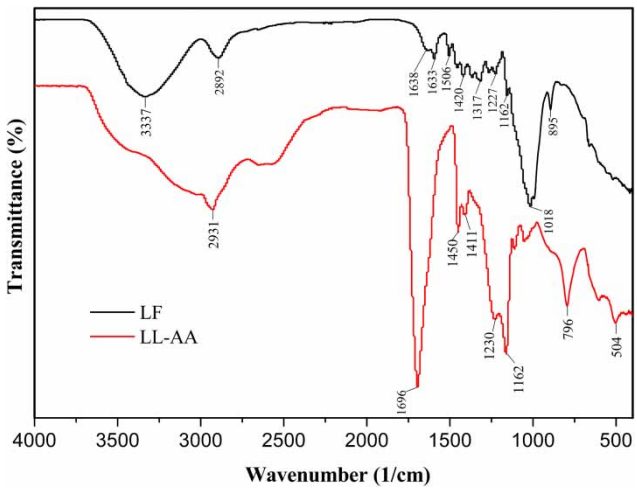

Figure 3 | Fourier transform infrared spectrometry (FTIR) of LF and LF-AA.

The surface chemical structures of pristine (LF) and modified LF (LF-AA) were studied by ATR-FTIR, as shown in Figure 3. For pristine LF, the peak 3,337 cm^{-1} corresponded to the stretching vibration of –OH and $–NH_2$ groups on the surface of LF. The absorption peaks at 2,892 and 1,638 cm^{-1} corresponded to the stretching vibrations of C–H bond and carbonyl stretching of para-substituted ketones or aryl aldehydes (Tarley & Arruda 2004). The peak at 1,162 cm^{-1} is assigned to asymmetric bridge of C–O–C stretching, and the peaks at 1,018 and 895 cm^{-1} correspond to C–H deformation and β-glucosidic linkage, respectively (Gupta *et al.* 2013). Compared with pristine LF, the FTIR–ATR spectra of LF-AA showed three new characteristic absorption peaks at 1,696, 1,450 and 1,162 cm^{-1}, which are related to the stretching vibration of C=O, stretching vibration and symmetrical stretching of –COO groups, respectively (Pourjavadi *et al.* 2010). All these results show that carboxyl groups have been successfully grafted to the surface of LF.

Batch study

Effect of pH

To evaluate the effect of pH, we studied the adsorption of Ce(III) over the pH range 1.0 to 6.0. As results displayed in Figure 4(a), the adsorption capacity of Ce(III) was increased with the pH increase from 1.0 to 6.0. Apparently, these results were thanks to the effective grafting between natural LF and carboxyl groups. The equilibrium pH values were also determined, and the maximum adsorption capacity was achieved at equilibrium pH 5.1 (corresponds to initial pH 6.0). To further study the adsorption mechanism, a zeta potential analysis of LF-AA was investigated. As shown in Figure 4(b), the surface of LF-AA was negatively charged, the zeta potential of LF-AA was near 0 at pH 1.0 and then becomes stronger with the rising of solution pH, which is beneficial for adsorbing metal cations. These phenomena can be explained as follows: At low pH, the concentration of H^+ is high and the surface of the adsorbents presents in carboxyl form (Ge *et al.* 2012). The lower adsorption efficiency at low pH may result from the strong coulomb repulsion and the competition between the H^+ and Ce(III). As expected, with the pH value increased, the adsorption capacity of LF-AA sharply increased and reaches a high level at higher pH values. At higher pH values, the weakly acidic carboxyl groups will be deprotonated and resulting in more negative binding sites; therefore, the attraction of positively charged metal ions would be enhanced, thus improving the adsorption capacity (Bayramoglu & Yakup Arica 2009; Badruddoza *et al.* 2011).

Effect of ionic strength and adsorption of different rare earth ions

Alkaline metal ions are often present together with rare earth ions in water systems. Therefore, studying the effect of solution ionic strength is of significance in adsorption process. The effect of ionic strength on the adsorption of Ce(III) was studied at pH 6.0 with NaCl as background electrolyte. The batch adsorption results are presented in Figure 4(c); the adsorption capacity of LF-AA was not greatly affected by the ionic strength, indicating that the binding affinity of Ce(III) with carboxyl groups is stronger than for sodium ions, and ion exchange is more prone to occur between Ce(III) and carboxylate of adsorbent surface. The adsorption performance of rare earth ions with different ionic radius was also studied at pH 6.0, as shown in Figure 4(d); LF-AA possessed different adsorption capacity towards different rare earth ions and followed the order Dy(III) > Ce(III) > La(III) > Eu(III) > Y(III), which suggests that LF-AA amount adsorbed is related to ionic radius.

Adsorption kinetics

Figure 5(a) reveals the effect of contact time on Ce(III) adsorption onto the adsorbent LF-AA under three initial concentrations (100 mg/L, 200 mg/L, 300 mg/L) at pH 6.0. It has a rapidly increasing speed for the first 50 min, which achieves most of the adsorption capacity, and then gradually moves into a slower stage as the contact time

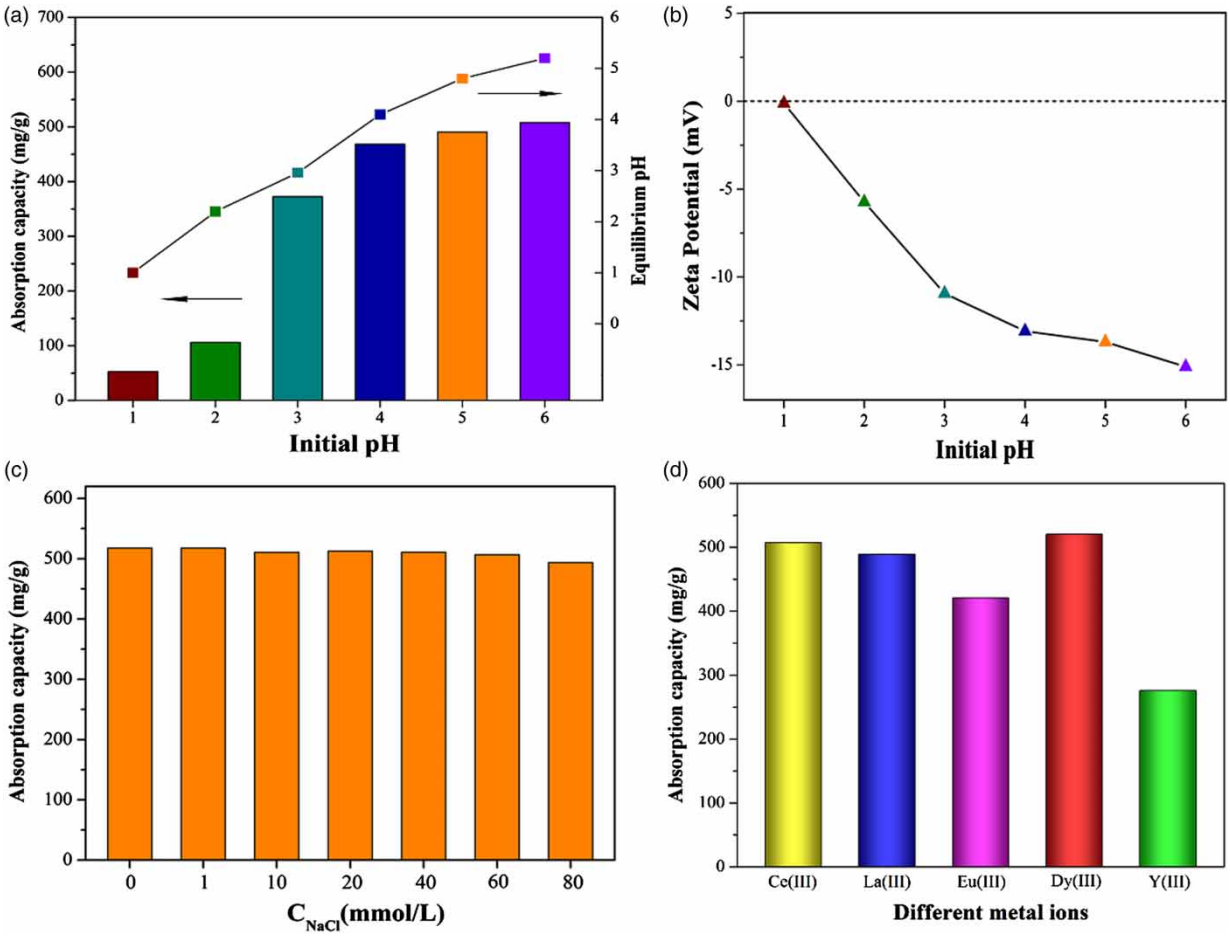

Figure 4 | Effect of pH (a) and ionic strength (c) on the adsorption capacity of LF-AA toward Ce(III). (b) The zeta potentials of the adsorbent at different pH values. (d) The adsorption of different rare earth ions.

increases until it reaches adsorption equilibrium. The adsorption capacities were equal to 190.2, 387.4 and 516.2 mg/g at initial concentrations of 100, 200, and 300 mg/L, respectively. This phenomenon could be attributed to the countless active sites (–COO– groups) from grafting and the porous structure of LF base. Specifically, metal cation was firstly migrated

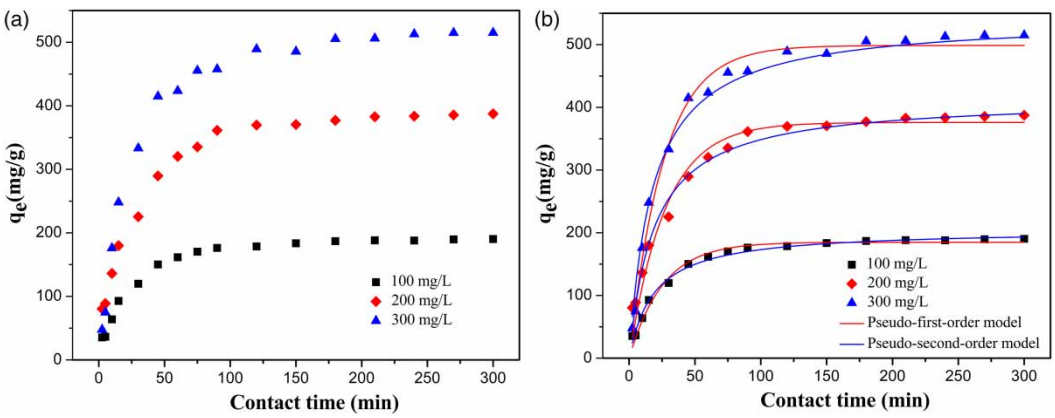

Figure 5 | (a) Effect of time on the adsorption of metal ions and (b) nonlinear fitting of pseudo-first-order and pseudo-second-order models.

Table 1 | Kinetic parameters of pseudo-first-order and pseudo-second-order kinetic models for Ce(III) adsorption onto LF-AA

		Pseudo-first-order model			Pseudo-second-order model		
C_0 (mg·L^{-1})	$q_{e,\ exp}$ (mg·g^{-1})	k_1 (min^{-1})	$q_{e,\ cal,1}$ (mg·g^{-1})	R^2	k_2 (g·mg^{-1}·min^{-1})	$q_{e,\ cal,2}$ (mg·g^{-1})	R^2
100	190.2	0.0393	184.9	0.9842	0.00026	192.1	0.9918
200	387.4	0.0366	376.0	0.9691	0.00016	394.6	0.9927
300	516.2	0.0383	498.7	0.9892	0.00011	523.7	0.9917

and adsorbed on the surface of LF-AA, which mainly resulted from ion exchange and charge neutralization. When the surface adsorption reached saturation, the rare earth cation would gradually diffuse to the interior of LF-AA and then be adsorbed on the interior of LF-AA, which made the subsequent diffusion (i.e. inner diffusion) more difficult; this stage should take a relatively long time (Ghaedi *et al.* 2011; Wang *et al.* 2014).

The pseudo-first-order and the pseudo-second-order plots for the adsorption of the Ce(III) on the LF-AA are shown in Figure 5 and the kinetic constants of these models are given in Table 1. It is clear that the R^2 of pseudo-second-order adsorption model was more close to 1 than pseudo-first-order model, and the values of $q_{e,exp}$ (experimental values of adsorption capacities) are closer to $q_{e,cal,2}$ (calculated by pseudo-second-order equation) than that of $q_{e,cal,1}$ (calculated by pseudo-first-order equation). This result suggests that the pseudo-second-order adsorption model was more suitable for the adsorption of Ce(III), and the metal ions adsorption onto LF-AA may take place through a chemical process involving valence forces through sharing or exchange of electrons (Li *et al.* 2015).

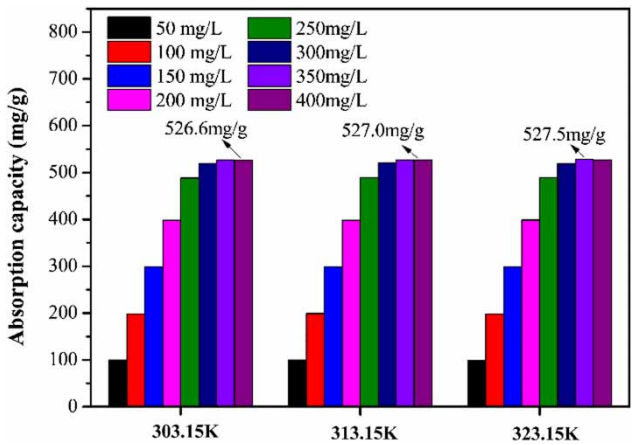

Figure 6 | Effect of temperature on the adsorption of Ce(III) onto LF-AA.

Adsorption isotherms

As an important parameter of heavy metal adsorption at liquid–solid interfaces, the effect of temperature (303.15, 313.15, and 323.15 K) on adsorption of Ce(III) onto LF-AA was examined at pH 6.0 as shown in Figure 6. The maximum adsorption capacity of Ce(III) was achieved at 323.15 K. The adsorption capacity led to an inconspicuous increase with the temperature increasing from 313.15 K to 323.15 K. Increasing adsorption temperature is known to enhance the possibility of interaction between metal ions and the adsorbent, and it is favorable for the transfer and diffusion of adsorbate from bulk solution to adsorbent surface. However, the increase of temperature may also cause greater mobility of the adsorbate molecules previously

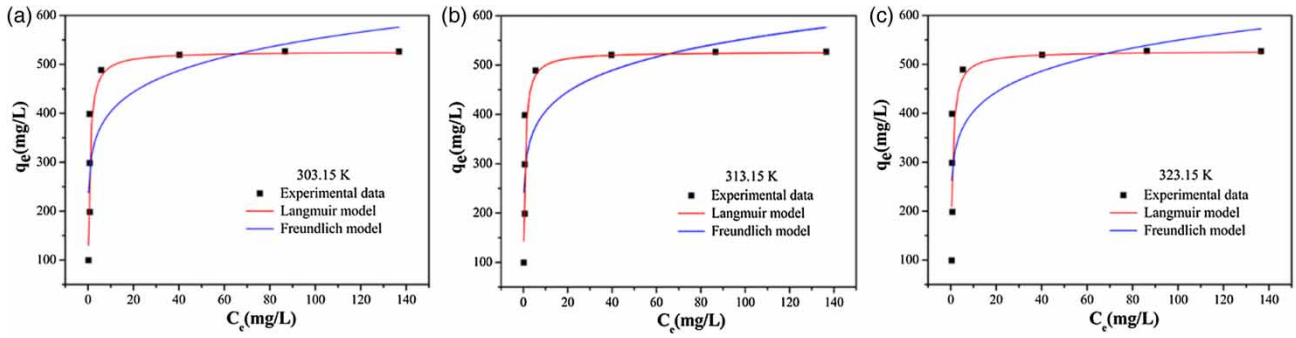

Figure 7 | Adsorption equilibrium isotherm data of Ce(III) onto LF-AA fitting to various isotherm equations.

Table 2 | Adsorption isotherm constants for Ce(III) adsorption onto LF-AA

	Langmuir			Freundlich		
T(K)	q_m (mg g^{-1})	k_L (L g^{-1})	R^2	k_F (mg$^{1-1/n}$ L$^{1/n}$ g^{-1})	1/n	R^2
303.15	526.31	1.61	0.9774	294.71	0.1362	0.7014
313.15	527.01	1.82	0.9800	298.77	0.1337	0.7011
323.15	527.27	1.63	0.9460	296.82	0.1338	0.6512

adsorbed (Li & Lei 2012; Li *et al.* 2015). It indicated that the temperature has no significant influences on adsorption of Ce(III) onto LF-AA based on the above two considerations.

The adsorption isotherm and non-linear fitting of the adsorption isotherm models are shown in Figure 7. The q_e of the metal ions was increased with increasing concentrations until reaching equilibrium. The parameters of Langmuir and Freundlich isotherm models were calculated and summarized in Table 2. Obviously, the Langmuir equation fitted the isotherm data well, with all R^2 value, more close to 1, which indicates that the binding sites of LF-AA are uniformly distributed on its surface, and the adsorption of Ce(III) is regarded as monolayer adsorption (Li *et al.* 2015). Comparison with several reported biomass adsorbents is listed in Table 3, revealing that LF-AA exhibits excellent adsorption ability for the recovery of Ce(III) from aqueous solutions.

Table 3 | Comparison of adsorption capacities of Ce(III) between various biomass adsorbents

Adsorbent	Adsorption capacity (mg/g)	Conditions	Reference
Pinus brutia leaf	17.24	pH 5; 303.15 K	Kütahyali *et al.* (2010)
Platanus orientalis leaf	32.05	pH 4; 303.15 K	Sert *et al.* (2008)
Crab shell	144.90	pH 4, 296.15	Vijayaraghavan & Balasubramanian (2010)
Tangerine peel	162.79	pH 5.0 K	Meisam (2013)
Corn style	180.20	4 h	Jaya *et al.* (2014)
Prawn carapace	218.30	6 h	Jaya *et al.* (2014)
Wheat straw	298.60	pH 5.6; 303.15 K	Zhou *et al.* (2016a)
LF-AA	527.50	pH 6.0; 323.15 K	This work

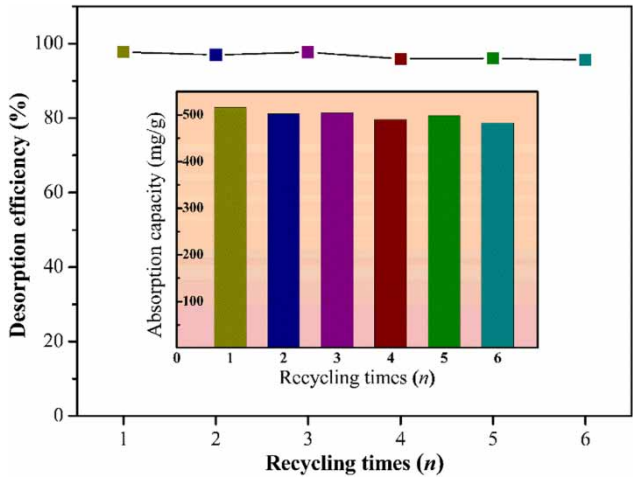

Figure 8 | Effect of cycle times on desorption efficiency and (inset) adsorption capacity.

Regeneration and reusability

The regeneration and reusability are important factors of a new adsorbent from a practical point of view. To evaluate the reusability of the adsorbent, six consecutive adsorption/desorption cycles were conducted and the results are presented in Figure 8. The adsorbent (LF-AA) achieved high and stable adsorption efficiency in the regeneration and reuse processes. Specifically, the total adsorption capacity of LF-AA for Ce(III) after six consecutive cycles decreased slightly from 515.8 to 482.7 mg/g, which is only a 6.40% reduction compared with the initial capacity of LF-AA, and it is still better than that for other polymeric absorbents that are freshly prepared. Moreover, desorption efficiency was also above 97.0% throughout the six cycles with 0.2 M HCl. Clearly, LF-AA in our study has good potential for repeated utilization for the adsorption and recycling of rare earth ions (Ce(III)) from water.

CONCLUSIONS

In this study, an efficient adsorbent was successfully synthesized on the basis of natural loofah sponge fiber via ultraviolet radiation grafting route. The LF-AA composites obtained were found to retain properties of their components, namely ideal structure for application (from LF), excellent adsorption/desorption capability for metal ions (from AA). In addition, the LF-AA exhibits excellent reuse

ability, with maximum adsorption capacity of 527.5 mg/g for Ce(III), which could be used as a reusable adsorbent with convenient conditions. According to the characterization analysis, the main adsorption mechanism should be ion exchange happening on the –COO– sites and then forming a bidentate chelate. Therefore, this adsorbent with excellent performances can be applied in the recovering of rare earth and other metal ions from water.

ACKNOWLEDGEMENTS

The authors are grateful for being jointly supported by Public Service Project of the Chinese Ministry of Land and Resources (201311024), Comprehensive Utilization Demonstration Base of Ganzhou Rare Earth Resource sponsored by Chinese Ministry of Land and Resources, Land Resources Geology Survey Projects of China and the Fundamental Research Funds for the Central Universities, China University of Geosciences (Wuhan) (CUGL150803).

REFERENCES

Altinisik, A., Gur, E. & Seki, Y. 2010 A natural sorbent, Luffa cylindrica for the removal of a model basic dye. *Journal of Hazardous Materials* **179** (1–3), 658–664.

Babula, P., Adam, V., Opatrilova, R., Zehnalek, J., Havel, L. & Kizek, R. 2008 Uncommon heavy metals, metalloids and their plant toxicity: a review. *Environmental Chemistry Letters* **6** (4), 189–213.

Badruddoza, A. Z., Tay, A. S., Tan, P. Y., Hidajat, K. & Uddin, M. S. 2011 Carboxymethyl-beta-cyclodextrin conjugated magnetic nanoparticles as nano-adsorbents for removal of copper ions: synthesis and adsorption studies. *Journal of Hazardous Materials* **185** (2–3), 1177–1186.

Basha, S., Murthy, Z. V. P. & Jha, B. 2009 Sorption of Hg(II) onto Carica papaya: experimental studies and design of batch sorber. *Chemical Engineering Journal* **147** (2–3), 226–234.

Bayramoglu, G. & Yakup Arica, M. 2009 Construction a hybrid biosorbent using Scenedesmus quadricauda and Ca-alginate for biosorption of Cu(II), Zn(II) and Ni(II): kinetics and equilibrium studies. *Bioresource Technology* **100** (1), 186–193.

Bilal, M., Shah, J. A., Ashfaq, T., Gardazi, S. M., Tahir, A. A., Pervez, A., Haroon, H. & Mahmood, Q. 2013 Waste biomass adsorbents for copper removal from industrial wastewater–a review. *Journal of Hazardous Materials* **263** (Pt 2), 322–333.

Binnemans, K., Jones, P. T., Blanpain, B., Van Gerven, T., Yang, Y., Walton, A. & Buchert, M. 2013 Recycling of rare earths: a critical review. *Journal of Cleaner Production* **51**, 1–22.

Brioschi, L., Steinmann, M., Lucot, E., Pierret, M. C., Stille, P., Prunier, J. & Badot, P. M. 2013 Transfer of rare earth elements (REE) from natural soil to plant systems: implications for the environmental availability of anthropogenic REE. *Plant & Soil* **366** (1–2), 143–163.

Chen, Z. 2011 Global rare earth resources and scenarios of future rare earth industry. *Journal of Rare Earths* **29** (1), 1–6.

Fan, G., Yuan, Z. & Zheng, H. 2004 Study on the effects of exposure to rare earth elements and health-responses in children aged 7–10 years. *Journal of Hygiene Research* **33** (1), 23–28.

Feng, L., Xiao, H., He, X., Li, Z., Li, F., Liu, N., Zhao, Y., Huang, Y., Zhang, Z. & Chai, Z. 2006 Neurotoxicological consequence of long-term exposure to lanthanum. *Toxicology Letters* **165** (2), 112–120.

Gao, Y., Zhang, S., Zhao, K., Wang, Z., Xu, S., Liang, Z. & Wu, K. 2015 Adsorption of La^{3+} and Ce^{3+} by poly-γ-glutamic acid crosslinked with polyvinyl alcohol. *Journal of Rare Earths* **33** (8), 884–891.

Ge, F., Li, M. M., Ye, H. & Zhao, B. X. 2012 Effective removal of heavy metal ions Cd^{2+}, Zn^{2+}, Pb^{2+}, Cu^{2+} from aqueous solution by polymer-modified magnetic nanoparticles. *Journal of Hazardous Materials* **211–212** (2), 366–372.

Ghaedi, M., Hassanzadeh, A. & Kokhdan, S. N. 2011 Multiwalled carbon nanotubes as adsorbents for the kinetic and equilibrium study of the removal of alizarin red S and morin. *Journal of Chemical & Engineering Data* **56** (5), 2511–2520.

Ghali, L., Msahli, S., Zidi, M. & Sakli, F. 2009 Effect of pre-treatment of Luffa fibres on the structural properties. *Materials Letters* **63** (1), 61–63.

Gupta, V. K., Agarwal, S., Singh, P. & Pathania, D. 2013 Acrylic acid grafted cellulosic Luffa cylindrical fiber for the removal of dye and metal ions. *Carbohydrate Polymers* **98** (1), 1214–1221.

Hameed, B. H. & Ahmad, A. A. 2009 Batch adsorption of methylene blue from aqueous solution by garlic peel, an agricultural waste biomass. *Journal of Hazardous Materials* **164** (2–3), 870–875.

Henriksson, Å. & Gatenhalm, P. 2002 Surface properties of CTMP fibers modified with xylans. *Cellulose* **9** (1), 55–64.

Jaroniec, M., Deryło, A. & Marczewski, A. 1983 The Langmuir-Freundlich equation in adsorption from dilute solutions on solids. *Monatshefte Fuer Chemie/Chemical Monthly* **114** (4), 393–397.

Jaya, S. V. C., Das, D. & Das, N. 2014 Optimization of parameters for cerium(III) biosorption onto biowaste materials of animal and plant origin using 5-level Box-Behnken design: Equilibrium, kinetic, thermodynamic and regeneration studies. *Journal of Rare Earths* **32** (8), 745–758.

Jordens, A., Cheng, Y. P. & Waters, K. E. 2013 A review of the beneficiation of rare earth element bearing minerals. *Minerals Engineering* **41**, 97–114.

Karlsson, J. O., Henriksson, Å., Michálek, J. & Gatenholm, P. 2000 Control of cellulose-supported hydrogel microstructures by three-dimensional graft polymerization of glycol methacrylates. *Polymer* **41** (4), 1551–1559.

Kato, K., Uchida, E., Kang, E.-T., Uyama, Y. & Ikada, Y. 2003 Polymer surface with graft chains. *Progress in Polymer Science* **28** (2), 209–259.

Kütahyali, C., Sert, Ş., Çetinkaya, B., Inan, S. & Eral, M. 2010 Factors affecting lanthanum and cerium biosorption on Pinus brutia leaf powder. *Separation Science and Technology* **45** (10), 1456–1462.

Langmuir, I. 1917 The constitution and fundamental properties of solids and liquids. *Journal of the Franklin Institute* **183** (1), 102–105.

Li, N. & Lei, X.-M. 2012 Adsorption of ponceau 4R from aqueous solutions by polyamidoamine–cyclodextrin crosslinked copolymer. *Journal of Inclusion Phenomena and Macrocyclic Chemistry* **74** (1–4), 167–176.

Li, J., Ren, Z., Ren, Y., Zhao, L., Wang, S. & Yu, J. 2014 Activated carbon with micrometer-scale channels prepared from luffa sponge fibers and their application for supercapacitors. *RSC Advances* **4** (67), 35789.

Li, M., Wang, S., Luo, W., Xia, H., Gao, Q. & Zhou, C. 2015 Facile synthesis and in situ magnetization of carbon-decorated lignocellulose fiber for highly efficient removal of methylene blue. *Journal of Chemical Technology & Biotechnology* **90** (6), 1124–1134.

Liu, H., Yang, J., Liu, Q., Jin, C., Wu, S., Lu, X., Zheng, L., Xi, Q. & Yuan, C. 2014 Lanthanum chloride impairs spatial memory through ERK/MSK1 signaling pathway of hippocampus in rats. *Neurochemical Research* **39** (12), 2479–2491.

Liu, C., Yan, C., Luo, W., Li, X., Ge, W. & Zhou, S. 2015 Simple preparation and enhanced adsorption properties of loofah fiber adsorbent by ultraviolet radiation graft. *Materials Letters* **157**, 303–306.

Madhukar Reddy, C., Deva Prasad Raju, B., John Sushma, N., Dhoble, N. S. & Dhoble, S. J. 2015 A review on optical and photoluminescence studies of RE^{3+} (RE = Sm, Dy, Eu, Tb and Nd) ions doped LCZSFB glasses. *Renewable and Sustainable Energy Reviews* **51**, 566–584.

Meisam, T. M. 2013 Biosorption of lanthanum and cerium from aqueous solutions using tangerine (Citrus reticulata) peel: equilibrium, kinetic, and thermodynamic studies. *Chemical Industry & Chemical Engineering Quarterly* **19** (1), 79–88.

Pourjavadi, A., Jahromi, P. E., Seidi, F. & Salimi, H. 2010 Synthesis and swelling behavior of acrylatedstarch-g-poly (acrylic acid) and acrylatedstarch-g-poly (acrylamide) hydrogels. *Carbohydrate Polymers* **79** (4), 933–940.

Sert, Ş., Kütahyali, C., İnan, S., Talip, Z., Çetinkaya, B. & Eral, M. 2008 Biosorption of lanthanum and cerium from aqueous solutions by Platanus orientalis leaf powder. *Hydrometallurgy* **90** (1), 13–18.

Tarley, C. R. & Arruda, M. A. 2004 Biosorption of heavy metals using rice milling by-products. Characterisation and application for removal of metals from aqueous effluents. *Chemosphere* **54** (7), 987–995.

Thakur, V. K. & Thakur, M. K. 2014 Processing and characterization of natural cellulose fibers/thermoset polymer composites. *Carbohydrate Polymers* **109**, 102–117.

Uda, T., Jacob, K. T. & Hirasawa, M. 2000 Technique for enhanced rare earth separation. *Science* **289** (5488), 2326–2329.

Vijayaraghavan, K. & Balasubramanian, R. 2010 Single and binary biosorption of cerium and europium onto crab shell particles. *Chemical Engineering Journal* **163** (3), 337–343.

Wang, S., Zhai, Y.-Y., Gao, Q., Luo, W.-J., Xia, H. & Zhou, C.-G. 2014 Highly efficient removal of Acid Red 18 from aqueous solution by magnetically retrievable chitosan/carbon nanotube: batch study, isotherms, kinetics, and thermodynamics. *Journal of Chemical & Engineering Data* **59** (1), 39–51.

Wu, D., Zhu, C., Chen, Y., Zhu, B., Yang, Y., Wang, Q. & Ye, W. 2012 Preparation, characterization and adsorptive study of rare earth ions using magnetic GMZ bentonite. *Applied Clay Science* **62–63**, 87–93.

Wübbeke, J. 2013 Rare earth elements in China: policies and narratives of reinventing an industry. *Resources Policy* **38** (3), 384–394.

Xie, F., Zhang, T. A., Dreisinger, D. & Doyle, F. 2014 A critical review on solvent extraction of rare earths from aqueous solutions. *Minerals Engineering* **56**, 10–28.

Yang, X. J., Lin, A., Li, X.-L., Wu, Y., Zhou, W. & Chen, Z. 2013 China's ion-adsorption rare earth resources, mining consequences and preservation. *Environmental Development* **8**, 131–136.

Yuan, Y., Zhou, S., Liu, Y. & Tang, J. 2013 Nanostructured macroporous bioanode based on polyaniline-modified natural loofah sponge for high-performance microbial fuel cells. *Environmental Science & Technology* **47** (24), 14525–14532.

Zhao, H., Cheng, Z., Cheng, J., Hu, R., Che, Y., Cui, Y., Wang, L. & Hong, F. 2011 The toxicological effects in brain of mice following exposure to cerium chloride. *Biological Trace Element Research* **144** (1–3), 872–884.

Zhou, S., Li, X., Shi, Y., Alshameri, A. & Yan, C. 2014 Preparation, characterization, and Ce(III) adsorption performance of poly (allylamine)/silica composite. *Desalination and Water Treatment* **56** (5), 1321–1334.

Zhou, Q., Yan, C. & Luo, W. 2016a Preparation of a novel carboxylate-rich wheat straw through surface graft modification for efficient separation of Ce(III) from wastewater. *Materials & Design* **97**, 195–203.

Zhou, Q., Yang, H., Yan, C., Luo, W., Li, X. & Zhao, J. 2016b Synthesis of carboxylic acid functionalized diatomite with a micro-villous surface via UV-induced graft polymerization and its adsorption properties for lanthanum(III) ions. *Colloids & Surfaces A Physicochemical & Engineering Aspects* **501**, 9–16.

First received 8 September 2016; accepted in revised form 20 February 2017. Available online 9 March 2017